Dynamics of an Insulating Skyrmion under a Temperature Gradient

Lingyao Kong[1] and Jiadong Zang[1,2,*]

[1]State Key Laboratory of Surface Physics and Department of Physics, Fudan University, Shanghai 200443, China
[2]Department of Physics and Astronomy, Johns Hopkins University, Baltimore, Maryland 21218, USA

(Received 5 February 2013; revised manuscript received 12 May 2013; published 8 August 2013)

We study the Skyrmion dynamics in thin films under a temperature gradient. Our numerical simulations show that both single and multiple Skyrmions in a crystal move towards the high temperature region, which is contrary to particle diffusion. Noticing a similar effect in the domain wall motion, we employ a theory based on magnon dynamics to explain this counterintuitive phenomenon. Unlike the temperature driven domain wall motion, the Skyrmion's topological charge plays an important role, and a transverse Skyrmion motion is observed. Our theory turns out to be in agreement with numerical simulations, both qualitatively and quantitatively. Our calculation indicates that a very promising Skyrmion dynamic phenomenon can be observed in experiments.

DOI: 10.1103/PhysRevLett.111.067203 PACS numbers: 75.70.Kw, 66.30.Lw, 75.10.Hk, 75.40.Mg

A Skyrmion is a topological configuration in which local spins wrap around the unit sphere an integer number of times [1]. After decades of theoretical discussions [2,3], it was recently observed in a bulk sample of MnSi [4]. This material is a typical helimagnet where the inversion asymmetry induced Dzyaloshinsky-Moriya (DM) interaction is significant; the latter plays an important role in generating Skyrmion configurations. The neutron scattering study [4] shows that Skyrmions perfectly pack themselves in triangle crystals as a compromise between the DM interaction and ferromagnetic Heisenberg exchange. However, due to the competition with the conical phase, the Skyrmion phase unfortunately survives only in a narrow window at finite temperatures [4]. More recently, a real space image in a $Fe_xCo_{1-x}Si$ thin film [5] demonstrated that a Skyrmion crystal phase can be considerably enlarged in two dimensions, and stable down to zero temperature [6–8]. Further exploration shows that Skyrmion phases are not only present in these two metallic materials, but also in insulating materials like Cu_2OSeO_3 [9] and $BaFe_{1-x-0.05}Sc_xMg_{0.05}O_{19}$ [10].

After the discovery of Skyrmion crystals, numerous efforts were devoted to the manipulations of Skyrmions. Because of their topological nature, Skyrmions remain stable against moderate perturbations. Therefore, controlling the motion of Skyrmions would allow for potential applications of Skyrmion physics. To this end, Skyrmion dynamics has been discussed in detail [11–13]. One well accepted way to control the motion of Skyrmions in metallic thin films is via a current. Unlike the regular domain wall motion driven by the current, the Skyrmion motion can occur at a tiny current threshold [14]. This advantage makes low-dissipative Skyrmion manipulation possible. An interesting question is if it is possible to drive the motion of insulating Skyrmions. If the answer is positive, one can thoroughly eliminate the dissipations from the conducting current.

In this Letter, we study the directional motion of insulating Skyrmions under a temperature gradient. Insulating materials help us to eliminate the influence of conduction electrons [14,15]. Interestingly, our study shows that Skyrmions unconventionally move towards high temperature regions, contrary to the usual Brownian motion. A Skyrmion as a large-size quasiparticle appears to have a negative diffusion coefficient. Followed by numerical simulations, a magnon assisted theory is employed to explain this novel phenomenon.

Numerical simulation.—To simulate the magnetization dynamics at finite temperature, the stochastic Landau-Lifshitz-Gilbert (LLG) approach is employed [16,17]. The effect of the thermal fluctuation at the temperature T is characterized by a random field $\mathbf{L}$ in addition to the usual LLG equation. The equation of motion is given by

$$\dot{\mathbf{m}} = -\gamma \mathbf{m} \times (\mathbf{H}_{\text{eff}} + \mathbf{L}) + \alpha \mathbf{m} \times \dot{\mathbf{m}}, \tag{1}$$

where $\gamma = g/\hbar$ is the gyromagnetic ratio and α is the Gilbert damping coefficient. The magnitude of the magnetization $\mathbf{m}$ is normalized to unity. In the case of ferromagnetic insulators α can be tiny, due to the absence of conduction electrons to dissipate the magnetization energy. $\mathbf{H}_{\text{eff}} = -\partial H/\partial \mathbf{m}$ is the effective field acting on the local magnetization $\mathbf{m}$. In order to eventually achieve thermal equilibrium, the dissipation-fluctuation relation $\langle L_\mu(\mathbf{r}, t) L_\nu(\mathbf{r}', t') \rangle = \xi \delta_{\mu\nu} \delta(\mathbf{r} - \mathbf{r}') \delta(t - t')$ is satisfied, where $\xi = \alpha a^2 k_B T/\gamma$ and a is the lattice constant. The average $\langle\,\rangle$ is taken over all the realizations of the fluctuation field. Here, a uniform but small temperature gradient is assumed. The thermal fluctuation of each spin is about $k_B T$, which is about $J/10$ in our simulation. As long as it is larger than the temperature difference between neighboring sites, local equilibrium can be established and this stochastic LLG approach is justified. In this case ξ, together with T, is a linear function of the position. In what follows, the temperature gradient is turned on longitudinally along the x direction. Numerically, the stochastic field $L_\mu(\mathbf{r}, t)$ is created by a random number generator with

the mean square controlled by the temperature, and the stochastic LLG equation [Eq. (1)] is integrated out in the deterministic Heun scheme [16], with a time step of $0.05\hbar/J$. The initial Skyrmion configurations are given by classical Monte Carlo updates followed by further relaxation realized by solving the LLG equation with a fourth order Runge-Kutta method [5].

We employed the standard model given by

$$H = \sum_{\langle ij \rangle} [-J\mathbf{m}_i \cdot \mathbf{m}_j + \mathbf{D}_{ij} \cdot (\mathbf{m}_i \times \mathbf{m}_j)] - \sum_i \mathbf{H} \cdot \mathbf{m}_i, \quad (2)$$

where the DM vector $\mathbf{D}_{ij} = D\hat{\mathbf{r}}_{ij}$ points from one local magnetization to the other. The magnetic field $\mathbf{H} = H\hat{z}$ is perpendicular to the film. H relates the real magnetic field h by $H = \mu_B h$. In the simulations, the Heisenberg exchange $J/k_B = 50$ K, and the strength of the DM interaction $D = 0.5J$. Note that in reality D is an order of magnitude smaller. The advantage of a large D in the current simulation is to reduce the Skyrmion radius and save the calculation resources. The lattice spacing a is 5 Å, and the full simulated sample size is $150a \times 50a$, which is much larger than the Skyrmion radius (about $5a$). Therefore the finite size effect is safely negligible. The Gilbert damping α is set to 0.1. This value is relatively larger than the realistic case, but it is helpful to obtain a relatively larger stochastic field to make the Skyrmion motions transparent in simulations.

The phase diagram of the Hamiltonian in Eq. (2) is already known [5,18]. The phase transition between the Skyrmion crystal and the ferromagnetic phase appears to be of first order and, therefore, the coexistence of both phases is observed. By tuning the external magnetic field H up to a critical value, the Skyrmion crystal is melted so that one can have a chance of obtaining a single Skyrmion on the thin film. The snapshots of a single Skyrmion are shown in Fig. 1(a). Once the magnetic field is further reduced, a perfect Skyrmion crystal is energetically favored [see Fig. 1(c)]. The color bars in these plots indicate the topological charge density $q = (1/4\pi)\mathbf{m} \cdot (\partial_x \mathbf{m} \times \partial_y \mathbf{m})$. The total topological charge $Q = \int d^2\mathbf{r} q$ counts the number of Skyrmions in the lattice.

As the simulation goes on, the single Skyrmion starts to move under the effect of the stochastic field. Although the instant velocity appears to be random, the overall velocity is nonzero. Quantitatively, we can define the center position $\mathbf{r}_c$ of the Skyrmion weighed by the topological charge: $\mathbf{r}_c = \int d^2\mathbf{r}\mathbf{m} \cdot (\partial_x \mathbf{m} \times \partial_y \mathbf{m})\mathbf{r} / \int d^2\mathbf{r}\mathbf{m} \cdot (\partial_x \mathbf{m} \times \partial_y \mathbf{m})$. Figure 2(a) shows a typical simulation result of the relation between the center position and the simulation time. At short time scales, the Skyrmion oscillates around an average position, in accordance with the thermal fluctuation. In the long run, the Skyrmion drifts directionally. The mean velocity is derived by averaging over 1000 simulated events. Its relation with the temperature gradient is shown in Fig. 2(b). The longitudinal velocity is proportional to the

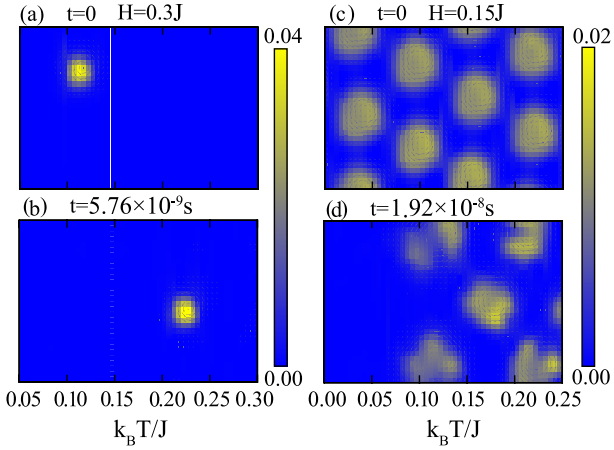

FIG. 1 (color online). Snapshots of Skyrmion motions. Color bars stand for the topological charge density q. (a) At the critical magnetic field of $H = 0.3J$, a single Skyrmion is generated. (b) Under a temperature gradient, it moves from low to high temperature. (c),(d) The Skyrmion crystal moves in a similar way under a lower magnetic field $H = 0.15J$.

temperature gradient. Meanwhile, the transverse velocity is nonzero and linear in temperature gradient as well, although the magnitude is one order of magnitude smaller than the longitudinal one. The transverse motion of the Skyrmion is another example of the Skyrmion Hall effect in analogy to the conventional Hall effect for electrons [11].

A surprising result is that the Skyrmion moves from the low temperature region to the high temperature one, as shown in Fig. 1(b). It is generally known that under a temperature gradient, particles like electrons should move to the cold terminal, due to the low density of hot particles at the cold end. This directional Brownian motion gives rise to various phenomena such as the Seebeck effect. Our result contradicts this physical picture. This effect even holds also for the entire Skyrmion crystal in which multiple Skyrmions are driven by the temperature gradient.

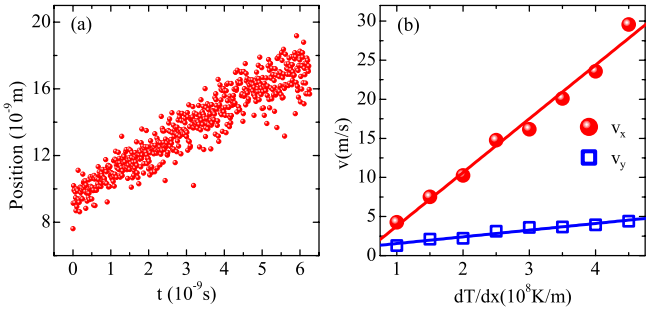

FIG. 2 (color online). (a) A typical simulation showing the Skyrmion's instantaneous longitudinal positions. Although it fluctuates under finite temperature, a forward average velocity is observed. (b) A linear scaling between the longitudinal velocity and the temperature gradient (circle). A nonvanishing v_y is also addressed (square), indicating the Skyrmion Hall effect.

As shown in Fig. 1(d), the whole crystal shifts towards high temperatures in a similar way. However, the crystal melts a little bit during the diffusion process.

Theory.—In order to understand the counterintuitive diffusion direction, a magnon assisted theory is employed [19]. In the simplest case of a ferromagnet polarized along $\hat{z}$, the spin's deviation (n_x, n_y) from its equilibrium direction is described by the presence of magnons. The magnon creation operator is $a^\dagger = (n_x - in_y)/\sqrt{2}$, and the magnon number operator is $\rho = a^\dagger a = (1/2)(n_x^2 + n_y^2)$. The spin component along the equilibrium direction is simply $n_z = \sqrt{1-(n_x^2+n_y^2)} \approx 1-\rho$. This result shows that each magnon carries one spin polarized antiparallel to the equilibrium direction. Therefore, once there is a Skyrmion under a temperature gradient, as shown in Fig. 3(a), the magnon as a low-lying excitation responds much more actively than the Skyrmion itself. As a typical quasiparticle, the magnon diffuses from the hot to the cold end in the usual way. Because of the antiparallel alignment of the spin, the magnon current provides a negative transfer torque on the Skyrmion. Because of the conservation of total angular momentum, the Skyrmion moves in the opposite way.

To quantitatively formulate this physical picture, let us decompose the local magnetizations into the slow mode $\mathbf{m}_s$ and the orthogonally fast mode $\mathbf{m}_f = \mathbf{m}_s \times \mathbf{n}$: $\mathbf{m} = (1-\mathbf{m}_f^2)^{1/2}\mathbf{m}_s + \mathbf{m}_f$. The slow mode is responsible for the equilibrium configuration of the Skyrmion. Substituting it into the continuum version of the Hamiltonian $H = \int d^2r[(1/2)J(\nabla\mathbf{m})^2 + (D/a)\mathbf{m}\cdot(\nabla\times\mathbf{m}) - (\mathbf{H}/a^2)\cdot\mathbf{m}]$ and keeping only the dominant terms arising from the fluctuations of the fast mode, one can obtain the following equation of motion for the slow mode [18,19]:

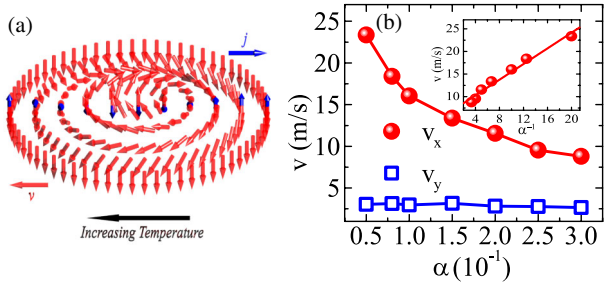

FIG. 3 (color online). (a) Sketch of physical picture for the Skyrmion motion towards high temperature. The long arrow (red) stands for the local magnetization constructing the Skyrmion configuration. The short arrow (blue) stands for the spin of the magnon, which points opposite to the local magnetization. Under a temperature gradient, the magnons move from the high temperature region to the low temperature one indicated by j, resulting in an opposite motion v for the Skyrmion. (b) The scaling of Skyrmion velocity with the Gilbert damping α. v_x is inversely proportional to α (circle and the inset). v_y is almost independent of α (square).

$$\dot{\mathbf{m}}_s = -\gamma J a^2 \mathbf{j}\cdot\nabla\mathbf{m}_s - \gamma\mathbf{m}_s\times\mathbf{L} + \alpha\mathbf{m}_s\times\dot{\mathbf{m}}_s, \quad (3)$$

where $j_i = \mathbf{m}_s\cdot(\mathbf{n}\times\partial_i\mathbf{n}) = i(\partial_i a^\dagger a - a^\dagger\partial_i a)$ is the magnon current induced by the temperature gradient. Note that the first term on the right-hand side of Eq. (3) is analogous to the spin transfer torque provided by the itinerant electrons in the adiabatic limit [11,20]. However, the sign is different in the two cases. The negative sign here corresponds to the negative transfer torque from the magnons.

Ignoring the deformation of the Skyrmion, the slow modes can be written in terms of the collective coordinates $\mathbf{u}(t)$ as $\mathbf{m}_s(r,t) = \mathbf{m}_s^0(\mathbf{r}-\mathbf{u}(t))$, where $\mathbf{m}_s^0$ is the ground configuration, and $\mathbf{u}(t)$ describes the position of the Skyrmion. Inserting it into Eq. (3) and integrating over the ground configuration, one finally obtains the equation of motion for the collective coordinates $Q\varepsilon^{ij}\dot{u}_j(t) = Q\gamma J a^2\varepsilon^{ij}j_j + 2\alpha\eta\dot{u}_i(t) + (\gamma/4\pi)\int d^2r\partial_i\mathbf{m}_s^0\cdot\mathbf{L}(\mathbf{r}+\mathbf{u},t)$, where the shape factor $\eta = (1/8\pi)\int d^2r\partial_i\mathbf{m}_s^0\times\partial_i\mathbf{m}_s^0$ is close to unity. We define a collective stochastic force l_i acting on the Skyrmion as a whole by $l_i(\mathbf{u},t) = \int d^2r\partial_i\mathbf{m}_s^0\cdot\mathbf{L}(\mathbf{r}+\mathbf{u},\mathbf{t})$, whose average then satisfies $\langle l_i(\mathbf{u},t)l_j(\mathbf{u}',t')\rangle = \xi'\delta_{ij}\delta(\mathbf{u}-\mathbf{u}')\delta(t-t')$ with a new mean square $\xi' = 8\pi\eta\xi = 8\pi\alpha\eta a^2 k_B T/\gamma$. The collective equation of motion resembles the standard Langevin equation. Let $P(\mathbf{r},t)$ be the probability to find the Skyrmion at position $\mathbf{r}$ and the time t. It thus satisfies the Fokker-Planck equation [21]: $(\partial P/\partial t) = -[\gamma J a^2 j_x - 2(\gamma/4\pi Q)^2(\partial_x\xi')]\partial_x P - \gamma J a^2 j_x 2\alpha\eta\partial_y P + (\gamma/4\pi Q)^2\times\xi'(\partial_x^2+\partial_y^2)P$. At the current stage, we are only interested in the lowest order traveling wave solution of the Fokker-Planck equation, namely $P(\mathbf{r},t) = P(\mathbf{r}-\mathbf{v}t)$. The last term provides nonlinearity: it thus broadens the wave package and can be neglected. Finally, we obtain the average velocity of the Skyrmion in both the longitudinal and transverse directions

$$v_x = \gamma J a^2 j_x - \frac{\gamma}{\pi Q^2}\alpha\eta a^2 k_B\frac{dT}{dx} \equiv v_x^M - v^B, \quad (4)$$

$$v_y = 2\alpha\eta v_x^M. \quad (5)$$

The contributions from the magnon and the Brownian motion are separable and are denoted, respectively, by $v_{x,y}^M$ and v^B. Equation (4) shows explicitly that their effects are completely opposite: the Skyrmion is pushed by the Brownian motion towards the cold terminal, while it is pulled back to the hot end by the magnon. On the other hand, as the temperature gradient is exerted along the x direction, the Brownian motion along the y direction vanishes on the average. Only the magnon effect contributes to the transverse velocity, which is a factor α smaller than the longitudinal one, agreeing with the numerical simulation in Fig. 2(b). This Hall effect of the Skyrmion motion is closely related to the topology of the Skyrmion texture

captured by the nonzero topological charge Q. Generally speaking, a directional transverse motion requires the breaking of time reversal symmetry. Here it is the dissipative damping α that breaks time reversal. Therefore one expects the proportionality between the transverse velocity and the Gilbert damping α.

Now it is important to evaluate the magnon current. To this end, we can apply a semiclassical approach with the relaxation time approximation [22]. The variation from the Bose-Einstein distribution f is given by $\delta f = \tau(\partial f/\partial\varepsilon)(\varepsilon/T)\mathbf{v}\cdot\nabla T$. τ is the relaxation time. The magnon current is consequently $j = a^2\int(d^2k/(2\pi)^2)k_x a_k^\dagger a_k = a^2\int(d^2k/(2\pi)^2)\tau k_x(\partial f/\partial\varepsilon)(\varepsilon/T)(\partial\varepsilon/\hbar\partial k_x)(dT/dx)$. In this simple evaluation, higher order processes such as magnon-magnon interactions are neglected so that τ is given by the Gilbert damping only. In the presence of a nonzero α, the magnon frequency acquires an imaginary value $\alpha\omega$. Therefore the magnon number decays exponentially as $\rho(t) \sim \exp(-2\alpha\omega t)$. The relaxation time is thus $\tau = 1/(2\alpha\omega)$. According to the work by Petrova and Tchernyshyov [23], linear dispersion is respected in the Skyrmion crystal, given by $\varepsilon\hbar\omega = (1/2)M_0 Da\gamma\hbar k \equiv s\hbar k$, where M_0 is the magnitude of the local spin. s is the effective velocity of the magnon. Finally one obtains the magnon current given by

$$j = j_x = \frac{\pi}{24}a^2\left(\frac{k_B}{\hbar s}\right)^2\frac{T}{\alpha}\frac{dT}{dx}. \tag{6}$$

This result indicates that the magnon current, as well as the Skyrmion velocity, is proportional to the temperature gradient. It is quite consistent with the numerical result in Fig. 2. This evaluation also explains why the magnon contribution is overwhelming in Eq. (4). The ratio between these two contributions is $v^B/v_x^M = (6/\pi)\alpha^2(D^2/Jk_BT)$. It is definitely a small number due to the small DM interaction and the tiny damping coefficient. The net effect of the Brownian motion is almost invisible in this case.

Another interesting conclusion from Eq. (6) is that j is inversely proportional to α. Consequently, the longitudinal Skyrmion velocity is also inversely proportional to α, while the transverse velocity is independent of α. In reality, dislocations or imperfections of the Skyrmion lattice may affect the magnon dispersion significantly. However, as long as the magnon-magnon interaction is negligible, the inverse proportionality between the longitudinal velocity and the Gilbert damping always holds. In the case of insulating helimagnets, as the magnetization energy can hardly be dissipated away, the Gilbert damping is tiny. The Skyrmion velocity can be quite large instead. In order to test this theory, we scaled the velocity with respect to α from the simulations, as shown in Fig. 3(b). A nice inverse proportionality between v_x and α is explicitly addressed. v_y remains almost the same for different α values. These results match well with our theory.

A similar magnon assisted theory was applied to the case of domain wall motion [17,19]. However, the difference brought by the topology of the Skyrmion is profound. In the derivation of the collective equation of motion, the quantization of topological charge Q is applied, which is the key feature of the Skyrmion. For the domain wall case, the total topological charge vanishes, so that this method does not apply. The collective equation of motion for the Skyrmion provides us a universal dynamics that weakly depends on the detailed structure of the Skyrmion. Furthermore, the Skyrmion stability allows us to treat it as a quasiparticle, so that the Fokker-Planck equation comes into play. The generalization from a 1D domain wall to a 2D Skyrmion crystal brings new phenomena such as the Skyrmion Hall effect.

Estimates.—For Cu_2OSeO_3, $J/k_B \sim 50$ K, $M_0 = 1/2$, and the spiral period is $\lambda \approx 2\pi Ja/D \sim 50$ nm [9]. Let $a \sim 5$ Å, thus $D/k_B \sim 3$ K, and the effective velocity $s \sim 15.6$ m/s. As a reasonable estimate, let $\alpha = 0.01$, then our theory gives $v_x \sim 1.2\times10^{-4}(dT/dx)$(m/s). In the numerical simulations, $v_x \sim 10^{-7}(dT/dx)$ for $\alpha = 0.1$. This 3 orders of magnitude difference can be perfectly fixed by noting a difference of a factor $\sim$10 in the DM interaction D, and another factor of 10 in the Gilbert damping α. This serves as a quantitative confirmation of our theory. Experimentally a reasonably large temperature gradient is about 1 K per millimeter [24], so that a velocity of 0.1 m/s can be achieved. This Skyrmion motion can be traced by real-space spectroscopies such as the Lorentz TEM. Another interesting issue is how to observe this phenomenon by transport measurements. As itinerant electrons are absent, signals of the topological Hall effect present in metallic Skyrmion crystals [25,26] are missing here. Probably the measurement technique of the spin Seebeck effect would come to help as a moving Skyrmion carries a spin current. There is no spin polarized electron current in this system, so that the signal of the moving Skyrmion would be dominant.

Compared to the domain wall motion, a peculiar advantage of the Skyrmion motion is its tiny pinning indicated by the small threshold current in the current driven case. This pinning results from impurities and lattice imperfections, which have basically the same level in insulating and metallic Skyrmion crystals. A low critical current of 10^6 A/m^2 is observed in MnSi [14], which corresponds to a theoretical velocity of 10^{-4} m/s [11]. Our estimate of the temperature gradient driven Skyrmion motion is far beyond this threshold; thus, it can be easily realized. The interaction between magnons and Skyrmions discussed here might open a new field of "Skyrmionic magnonics."

We are grateful for insightful discussions with A. Abanov, Cosimo Bambi, S. X. Huang, N. Nagaosa, V. Vakaryuk, O. Tchernyshyov, Y. Tserkovnyak, and Hui Wang. This work was supported in part by the Theoretical

Interdisciplinary Physics and Astrophysics Center and by the U.S. Department of Energy, Office of Basic Energy Sciences, Division of Materials Sciences and Engineering under Award No. DEFG02-08ER46544, and the Fudan Research Program on Postgraduates.

*jiadongzang@gmail.com

[1] T. H. R. Skyrme, Proc. R. Soc. A **260**, 127 (1961); Nucl. Phys. **31**, 556 (1962).
[2] A. N. Bogdanov and D. A. Yablonskii, Sov. Phys. JETP **68**, 101 (1989).
[3] U. K. Rößler, A. N. Bogdanov, and C. Pfleiderer, Nature (London) **442**, 797 (2006).
[4] S. Mühlbauer, B. Binz, F. Joinetz, C. Pfleiderer, A. Rosch, A. Neubauer, R. Georgii, and P. Böni, Science **323**, 915 (2009).
[5] X. Z. Yu, Y. Onose, N. Kanazawa, J. H. Park, J. H. Han, Y. Matsui, N. Nagaosa, and Y. Tokura, Nature (London) **465**, 901 (2010).
[6] S. D. Yi, S. Onoda, N. Nagaosa, and J. H. Han, Phys. Rev. B **80**, 054416 (2009).
[7] U. K. Rößler, A. A. Leonov, and A. N. Bogdanov, arXiv:1009.4849.
[8] J. H. Han, J. Zang, Z. Yang, J. H. Park, and N. Nagaosa, Phys. Rev. B **82**, 094429 (2010).
[9] S. Seki, X. Z. Yu, S. Ishiwata, and Y. Tokura, Science **336**, 198 (2012).
[10] X. Yu, M. Mostovoy, Y. Tokunaga, W. Zhang, K. Kimoto, Y. Matsui, Y. Kaneko, N. Nagaosa, and Y. Tokura, Proc. Natl. Acad. Sci. U.S.A. **109**, 8856 (2012).
[11] J. Zang, M. Mostovoy, J. H. Han, and N. Nagaosa, Phys. Rev. Lett. **107**, 136804 (2011).
[12] T. Schulz, R. Ritz, A. Bauer, M. Halder, M. Wagner, C. Franz, C. Pfleiderer, K. Everschor, M. Garst, and A. Rosch, Nat. Phys. **8**, 301 (2012).
[13] M. Mochizuki, Phys. Rev. Lett. **108**, 017601 (2012).
[14] F. Jonietz *et al.*, Science **330**, 1648 (2010).
[15] K. Everschor, M. Garst, B. Binz, F. Jonietz, S. Mühlbauer, C. Pfleiderer, and A. Rosch, Phys. Rev. B **86**, 054432 (2012).
[16] J. L. García-Palacios and F. J. Lázaro, Phys. Rev. B **58**, 14937 (1998).
[17] D. Hinzke and U. Nowak, Phys. Rev. Lett. **107**, 027205 (2011).
[18] See Supplemental Material at http://link.aps.org/supplemental/10.1103/PhysRevLett.111.067203 for the phase diagram and derivation of Eq. (3).
[19] A. A. Kovalev and Y. Tserkovnyak, Europhys. Lett. **97**, 67002 (2012).
[20] G. Tatara, H. Kohno, and J. Shibata, Phys. Rep. **468**, 213 (2008).
[21] H. Risken, *The Fokker-Planck Equation* (Springer-Verlag, Berlin, 1989), 2nd ed.
[22] N. W. Ashcroft and N. D. Mermin, *Solid State Physics* (Saunders College, Philadelphia, 1976).
[23] O. Petrova and O. Tchernyshyov, Phys. Rev. B **84**, 214433 (2011).
[24] K. Uchida, S. Takahashi, K. Harii, J. Ieda, W. Koshibae, K. Ando, S. Maekawa, and E. Saitoh, Nature (London) **455**, 778 (2008).
[25] A. Neubauer, C. Pfleiderer, B. Binz, A. Rosch, R. Ritz, P. Niklowitz, and P. Böni, Phys. Rev. Lett. **102**, 186602 (2009).
[26] S. X. Huang and C. L. Chien, Phys. Rev. Lett. **108**, 267201 (2012).